AMERICAN SOCIETY FOR MICROBIOLOGY | Infection and Immunity®

HOST RESPONSE AND INFLAMMATION

Schistosoma mansoni Worm Infection Regulates the Intestinal Microbiota and Susceptibility to Colitis

Achilleas Floudas,[a] Gabriella Aviello,[a]* Christian Schwartz,[a] Ian B. Jeffery,[b] Paul W. O'Toole,[b] Padraic G. Fallon[a]

[a]Trinity Biomedical Sciences Institute, School of Medicine, Trinity College Dublin, Dublin, Ireland
[b]School of Microbiology and APC Microbiome Institute, University College Cork, Cork, Ireland

ABSTRACT Infection with parasite helminths induces potent modulation of the immune system of the host. Epidemiological and animal studies have shown that helminth infections can suppress or exacerbate unrelated autoimmune, allergic, and other inflammatory disorders. There is growing evidence that helminth infection-mediated suppression of bystander inflammatory responses is influenced by alterations in the intestinal microbiome modulating metabolic and immune functions of the infected host. We analyzed the fecal microbiota of mice infected with adult male *Schistosoma mansoni* worms, which are less susceptible to experimental colitis, and male- and female-worm-infected mice, which are highly sensitive to colitis. While both groups of infected mice developed a disrupted microbiota, there were marked alterations in mice with male and female worm infections. Antibiotic-treated recipients that were cohoused with both types of *S. mansoni* worm-infected mice acquired a colitogenic microbiome, leading to increased susceptibility to experimental colitis. Following anthelmintic treatment to remove worms from worm-only-infected mice, the mice developed exacerbated colitis. This study provides evidence that adult male *S. mansoni* worm infection modulates the host's immune system and suppresses bystander colitis while limiting dysbiosis of the host's intestinal microbiome during infection.

KEYWORDS helminth, microbiome

Schistosomiasis is among the most common parasitic helminth diseases, with over 200 million people infected worldwide (1). This remarkable prevalence reflects the long-lasting coevolution of *Schistosoma* with humans. In order to achieve chronic, often decades-long, infections allowing the completion of the parasite's life cycle while causing low mortalities of infected hosts, schistosomes have developed multiple mechanisms to manipulate the host's innate and adaptive immune systems (2). Immunomodulation by schistosomes has been shown to not only benefit the parasite but also ameliorate unrelated inflammatory diseases through the initiation of regulatory mechanisms (3, 4).

Schistosoma mansoni chronically infects humans for ~10 years, during which time the intestine and systemic immunity endure constant exposure to controlled tissue inflammation. *S. mansoni* adult male and female worms reside in the mesenteric vasculature where they pair, mate, and lay ~350 eggs per worm pair in the blood each day. These eggs must translocate through the intestinal wall to be excreted in the feces (5). This process of intestinal egg granuloma formation and excretion by *S. mansoni* is mediated by the immune system of the infected host (6). Therefore, *S. mansoni* infection modulates immunity to achieve a state of homeostasis facilitating controlled inflammation of the intestinal wall. We have previously shown that infection of mice with *S. mansoni* male and female worms (MF infection) increases susceptibility to colitis in a preclinical experimental model of inflammatory bowel disease (IBD) while, in

Citation Floudas A, Aviello G, Schwartz C, Jeffery IB, O'Toole PW, Fallon PG. 2019. *Schistosoma mansoni* worm infection regulates the intestinal microbiota and susceptibility to colitis. Infect Immun 87:e00275-19. https://doi.org/10.1128/IAI.00275-19.

Editor De'Broski R. Herbert, University of Pennsylvania

Address correspondence to Padraic G. Fallon, pfallon@tcd.ie.

* Present address: Gabriella Aviello, The Rowett Institute, University of Aberdeen, Aberdeen, United Kingdom.

A.F. and G.A. are co-first authors.

Received 9 April 2019
Returned for modification 6 May 2019
Accepted 22 May 2019

Accepted manuscript posted online 28 May 2019
Published 23 July 2019

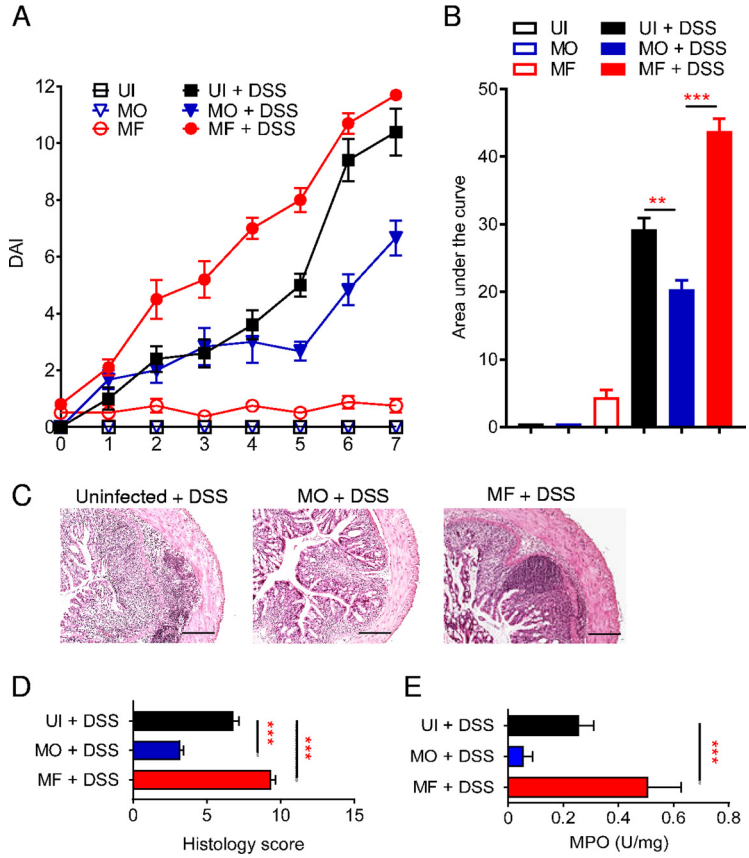

FIG 1 Ameliorated colitis in mice infected with male *S. mansoni* adult worms. (A) Colitis disease activity index (DAI) for mice infected with male-only (MO) or male-female (MF) *S. mansoni* worms or uninfected (UI) controls receiving DSS-water (filled symbols) or water (empty symbols). (B) Area under the curve analysis for DAI score over time of indicated groups of mice. (C and D) Representative H&E-stained histological sections of distal colon samples for the indicated groups and relative histological scores. (E) Myeloperoxidase (MPO) activity for the indicated groups of mice. Data are representative of >3 independent experiments and are presented as means ± SEM (3 to 6 mice per group). Statistical difference between groups was determined using one-way ANOVA followed by Tukey's multiple-comparison test. **, $P < 0.01$; ***, $P < 0.001$. Scale bar, 200 μm.

marked contrast, mice infected with male-only *S. mansoni* worms (MO infection), and thus without the intestinal immunopathology caused by eggs, experienced amelioration of colon inflammation (7).

Increasing evidence highlights the complexity and importance of the gut microbiome and the interactions between commensal bacteria and the host's immune system in health and disease (8). Alterations in the intestinal microbiota, known as dysbiosis, exert detrimental effects on the host's health by greatly influencing metabolic pathways and susceptibility to noninfectious diseases (9). In helminth-infected mice the interplay of modulation of the host's microbiome, metabolism, and immunity have been shown to impact unrelated inflammatory processes (10–12). In this study, we investigated if male-only or male and female *S. mansoni* infections of mice altered the composition of the intestinal microbiome and thereby modulated the susceptibility of infected mice to experimental colitis.

RESULTS

Mice with *S. mansoni* male-only worm infections show reduced susceptibility to DSS-induced colitis. In the dextran sulfate sodium (DSS) model of acute ulcerative colitis in BALB/c strain mice, ingestion of DSS causes intestinal epithelial damage and barrier disruption leading to inflammation and progression to marked colitis (Fig. 1). DSS-treated mice develop progressive signs of disease, with an elevation in the disease

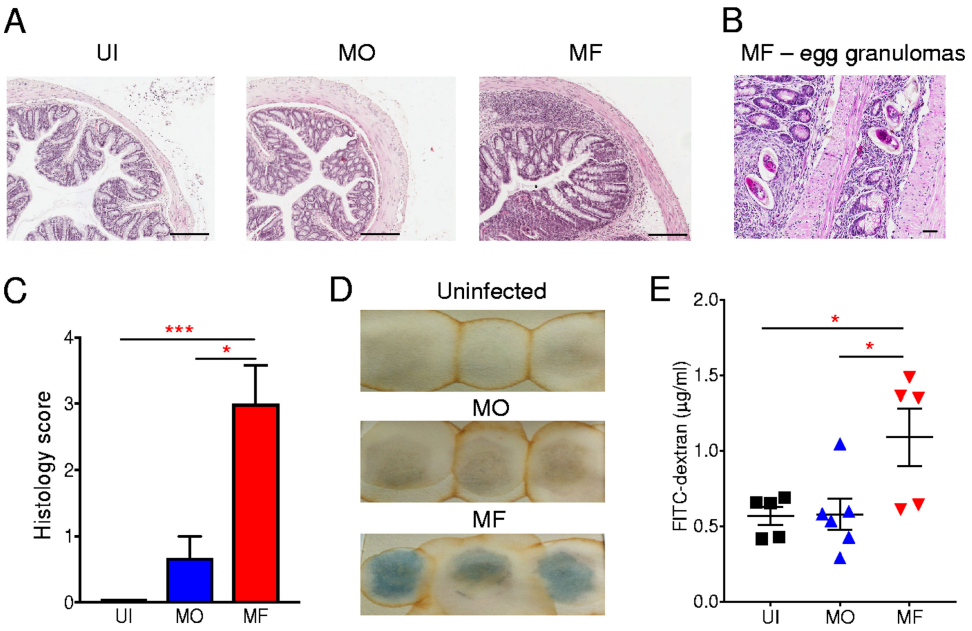

FIG 2 Compromised intestinal epithelial barrier in MF- but not MO-infected mice. (A) Representative H&E-stained histological sections of distal colon samples from uninfected (UI), male-only (MO)-infected, and male-female (MF)-infected mice. (B) Representative H&E-stained histological sections of distal colon samples from MF-infected mice showing the presence of egg granulomas. (C) Histological score of distal colon samples of indicated groups of mice. (D) Images of occult blood detection (blue) in fecal samples of the indicated groups of mice (3 mice per group). (E) Detection of FITC-labeled dextran in the plasma of the indicated groups of mice. Symbols represent individual mice. Data are representative of 3 independent experiments and are presented as means ± SEM (3 to 6 mice per group). Statistical differences between groups was determined by one-way ANOVA followed by Tukey's multiple-comparison test. *, $P < 0.05$, and ***, $P < 0.001$. Scale bars: 200 μm (A) and 40 μm (B).

activity index (DAI), reflecting loss of body weight and development of diarrhea with the presence of blood in the feces (Fig. 1A and B). These signs of colitis in mice are associated with epithelial erosion, crypt damage, and inflammatory cell infiltration in the lamina propria (Fig. 1C and D). Mice infected with male-only *S. mansoni* worms (MO) are partially resistant to DSS-induced colitis (7), with infected mice having a significant decrease in DAI score ($P < 0.01$ to 0.001), in colon tissue damage ($P < 0.001$), and in myeloperoxidase (MPO) activity ($P < 0.001$) compared to levels in control uninfected (UI) mice (Fig. 1A to E). In contrast, male-female *S. mansoni* (MF)-infected mice developed more severe colitis after DSS treatment (Fig. 1).

In other mouse models of inflammation, MO infections attenuated inflammation, anaphylaxis, and allergen-induced lung inflammation, while mice with conventional MF infections were more susceptible to disease (13, 14). Mice with MF infections are characterized by a type 2-biased immune response (2), and MO-infected mice also develop a type 2-dominated response, albeit one less pronounced than that of MF-infected mice, with elevated interleukin-4 (IL-4) and IL-10 and reduced gamma interferon (IFN-γ) production from spleen cells relative to levels from splenocytes from uninfected mice (13). In the context of intestinal immunity, activated mesenteric lymph node cells isolated from both infected groups had elevated IL-4, IL-10, and IL-17 and reduced IFN-γ production relative to cells from uninfected mice, with MF-infected cells producing significantly higher quantities of IL-4 and IL-17 ($P < 0.05$) than those of MO-infected mice (see Fig. S1 in the supplemental material). Therefore, mice with a male-only worm infection have a Th2 and Th17 bias in the intestinal lymph node cells that is less pronounced than that in MF-infected mice. During an MF infection, the eggs that are deposited in mesenteric vasculature transit via egg granulomas through the intestinal wall to be excreted in the gut lumen and feces. This process damages the colon (Fig. 2A), with granuloma formation around the eggs present in the intestine (Fig. 2B). This egg-induced damage to the intestines of MF-infected mice is evidenced by

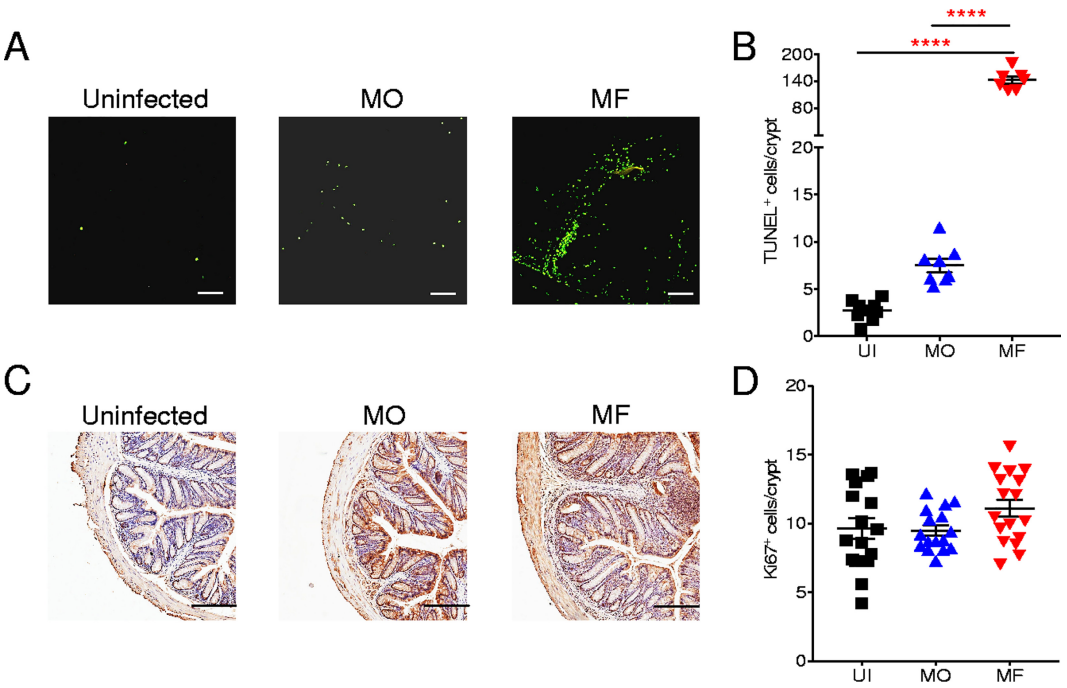

FIG 3 Increased intestinal epithelial apoptosis in MF- but not MO-infected mice. (A) Representative images of TUNEL assay for the identification of late-apoptotic cells (green) in distal colon samples from uninfected (UI), male-only (MO)-infected, and male-female (MF)-infected mice. (B) TUNEL-positive cells per crypt for the indicated groups of mice. (C) Representative images of Ki-67-positive cells per crypt. (D) Ki-67-positive cells per crypt. For both TUNEL and Ki-67 assays, 2 to 3 sections per mouse were used. Symbols represent individual mice. Data are presented as means ± SEM of from 7 to 17 mice. Statistical difference between groups was determined using one-way ANOVA followed by Tukey's multiple-comparison test. ****, $P < 0.0001$. Scale bar, 200 μm.

significantly ($P < 0.001$) marked colon pathology, including increased infiltration of leukocytes, submucosal inflammation, and ulcerations (Fig. 2C), as well as the presence of blood within the feces (Fig. 2C and D). Indeed, this subclinical colon damage in MF-infected mice is associated with the development of severe colitis after DSS exposure (Fig. 1), as reported previously (7). In contrast, MO-infected mice, which do not produce eggs, have no significant colon damage (Fig. 2A and C), which was reflected by the absence of blood in the feces (Fig. 2D).

To further address the integrity of the intestinal barrier of infected mice, fluorescein isothiocyanate (FITC)-labeled dextran was administered orally in order to quantify intestinal leakage. A significantly ($P < 0.05$) higher FITC-dextran level was detected in plasma of MF-infected mice than in plasma samples of MO-infected or UI control mice, indicating increased epithelial barrier permeability in MF-infected mice (Fig. 2E). To characterize the damage to the intestinal epithelial barrier during infection with *S. mansoni*, we performed a terminal deoxynucleotidyltransferase-mediated dUTP-biotin nick end labeling (TUNEL) assay for the detection of late-apoptotic cells in colonic tissue from *S. mansoni*-infected mice or uninfected controls (Fig. 3A and B). While there was a significant ($P < 0.0001$) increase in apoptotic cells in colon sections of MO-infected mice, the level of cell apoptosis was 30-fold higher in mice with MF infection (Fig. 3B). Furthermore, proliferation of cells in colon crypts was evaluated (Fig. 3C), with all groups having comparable cell proliferation levels (Fig. 3D). These data demonstrate that a conventional MF infection contributes to the increased susceptibility to DSS-induced colitis through the deposition of eggs that transit through the intestinal wall, leading to some colon damage and intestinal leakage. In contrast, a male-only worm infection does not alter the functional integrity of the colon, and these infected mice show reduced susceptibility to DSS-induced colitis.

***S. mansoni*-infected mice harbor a colitogenic microbiota.** Mice with MO or MF infections have contrasting differences in susceptibilities to DSS-induced colitis. Impor-

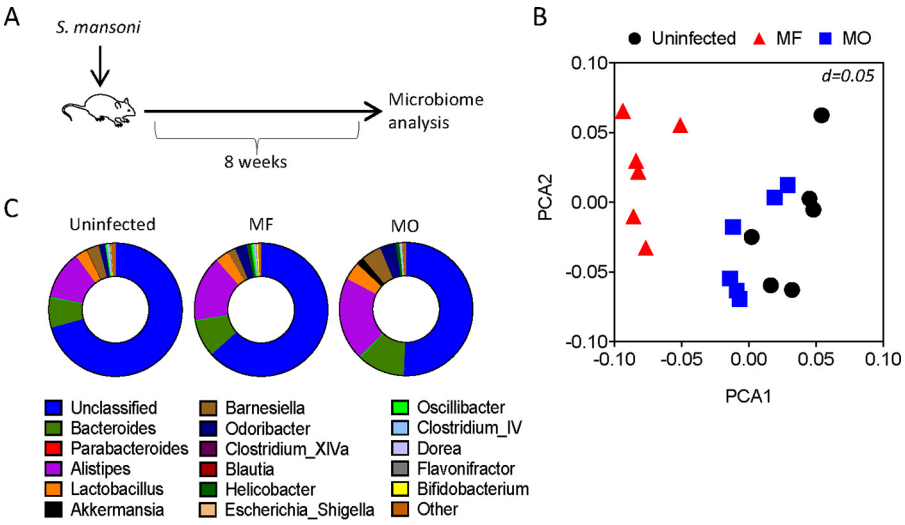

FIG 4 Effect of *S. mansoni* infections on intestinal microbial community. (A) Experimental design for the analysis of the intestinal microbiota following MO or MF infection. (B) Principal coordinate analysis (PCoA) for the fecal microbiota of the indicated groups of mice (6 mice per group). Each symbol represents an individual mouse. (C) Pie charts of the 16 common most abundant genera for the indicated groups of mice (6 mice per group).

tantly, the severity of disease in the DDS model of colitis is strictly dependent on the diversity of the gut microbiome of the mice (15, 16). We therefore analyzed the intestinal microbiota composition of MF- and MO-infected mice. Fecal samples were recovered from infected mice at 8 weeks postinfection, when DSS-induced colitis studies were performed, and from age- and sex-matched uninfected controls (Fig. 4A). Principal coordinate analyses (PCoA) of amplified 16S bacterial rRNA sequences extracted from fecal pellets revealed a distinct and significant clustering between the microbiota of MF-infected mice compared to that of MO-infected mice ($P = 0.032$) and uninfected controls ($P = 0.001$; Spearman distance, multivariate analysis of variance [MANOVA] methodology using the adonis function in the vegnan package in R) (Fig. 4B). While the fecal microbiota of MO-infected mice tended to separate from the microbiota of uninfected control mice, there was no clear demarcation between the groups (Fig. 4B). The average relative abundances of the most common identified genera highlighted the differences in species between groups, with increases in *Alistipes* and *Bacteroides* genera in the infected mice (Fig. 4C).

In order to further study the intestinal microbiota during *S. mansoni* infection, antibiotic-treated uninfected wild-type (WT) mice were cohoused for 3 weeks with *S. mansoni*-infected mice to repopulate the WT mice with the intestinal microbiome of infected animals (Fig. 5A). Antibiotic treatment profoundly altered the intestinal bacterial composition compared to that of untreated control mice (Fig. S2A). Importantly, following cohousing to induce fecal transfer of control (microbiome donor) mice to antibiotic-treated (microbiome recipient) mice, the recipients acquired the microbiome of the donors (Fig. S2B and C). Serum samples of antibiotic-treated WT mice cohoused with MO- and MF-infected mice were analyzed for presence of parasite antigen-specific (soluble egg antigen [SEA] or adult worm antigen [AW]) antibody responses, with serum from MF-infected mice serving as positive control. Following cohousing of UI and MO-infected [UI(MO)] mice, animals did not develop antibodies to SEA or AW, while UI(MF) mice produced antibodies to SEA (Fig. S3). As eggs would be excreted in feces of MF-infected but not MO-infected mice, coprophagy may have primed for a SEA-specific antibody response in uninfected mice cohoused with MF-infected mice.

The intestinal microbiomes of uninfected mice cohoused with MO-infected [UI(MO)] or MF-infected [UI(MF)] microbiome donors were similar and significantly ($P = 0.001$ and 0.002, respectively) distinct from the microbiome of mice cohoused with UI [UI(UI)]

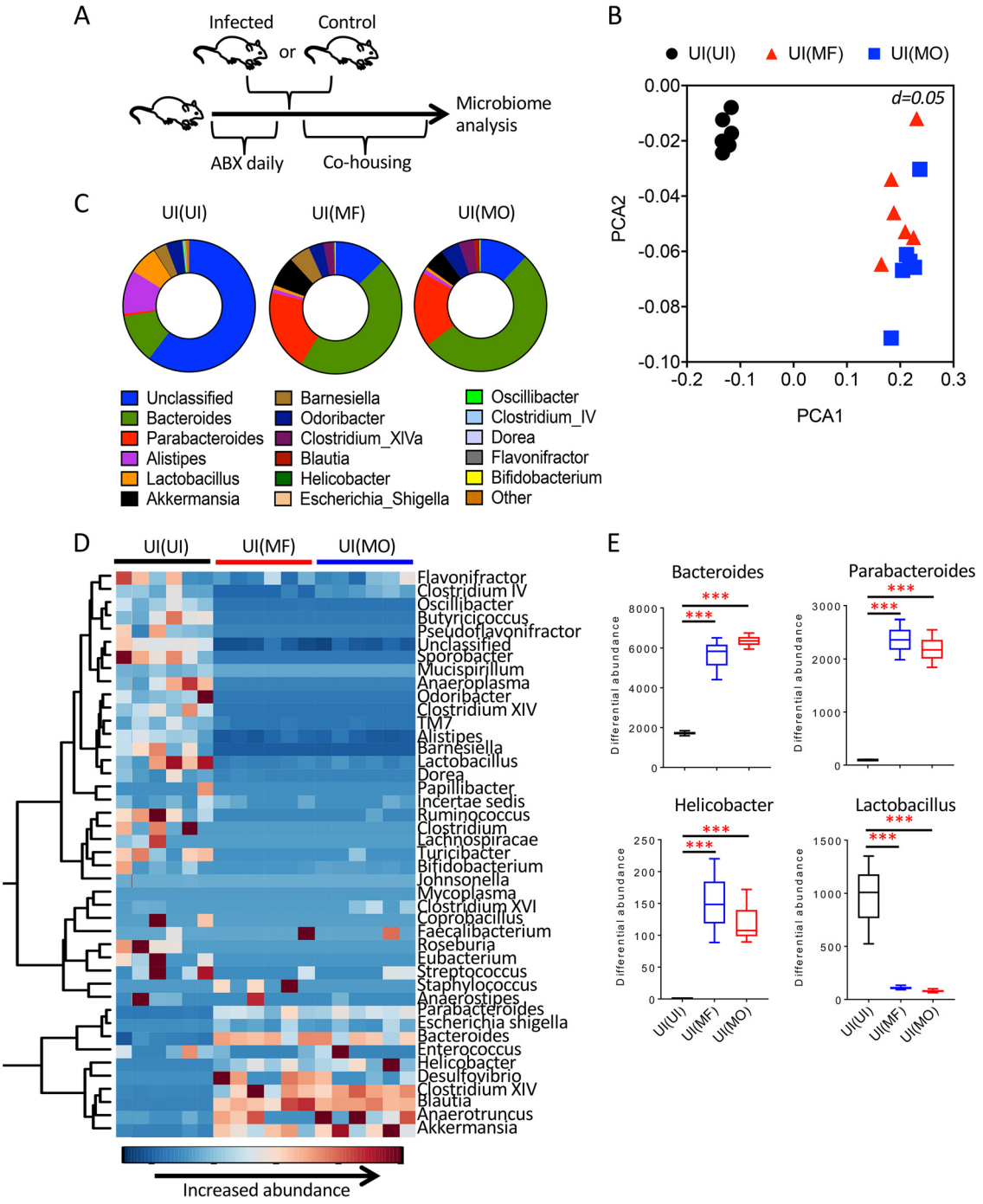

FIG 5 Analysis of fecal microbiome of recipient mice cohoused with *S. mansoni*-infected mice. (A) Experimental design of microbiome transfer from *S. mansoni*-infected or uninfected (control) mice to microbiome recipient uninfected mice treated with antibiotics (ABX). (B) Principal coordinate analysis (PCoA) of the microbiota from mice cohoused with uninfected [UI(UI)] mice, MF-infected [UI(MF)] mice, or MO-infected [UI(MO)] mice (6 mice per group). (C) Pie charts of the 16 common most abundant genera for the indicated groups of mice (6 mice per group). (D) Hierarchical clustering dendrogram of bacterial genus profiles for the indicated groups of mice (6 mice per group). (E) Comparison of differential abundances for *Parabacteroides*, *Bacteroides*, *Helicobacter*, and *Lactobacillus* for the indicated groups of mice. Data are presented as means ± SEM. Statistical difference between groups was determined using two-way ANOVA followed by Tukey's multiple-comparison test. ***, $P < 0.001$.

controls (Fig. 5B). There were also changes in species prevalences between UI(MO) and UI(MF) mice and UI(UI) mice (Fig. 5C), with an increase in closely hierarchically clustered bacterial genera (Fig. 5D). Of potential interest, the genera *Parabacteroides*, *Bacteroides*, and *Helicobacter*, which are associated with aggravated experimental colitis (17, 18),

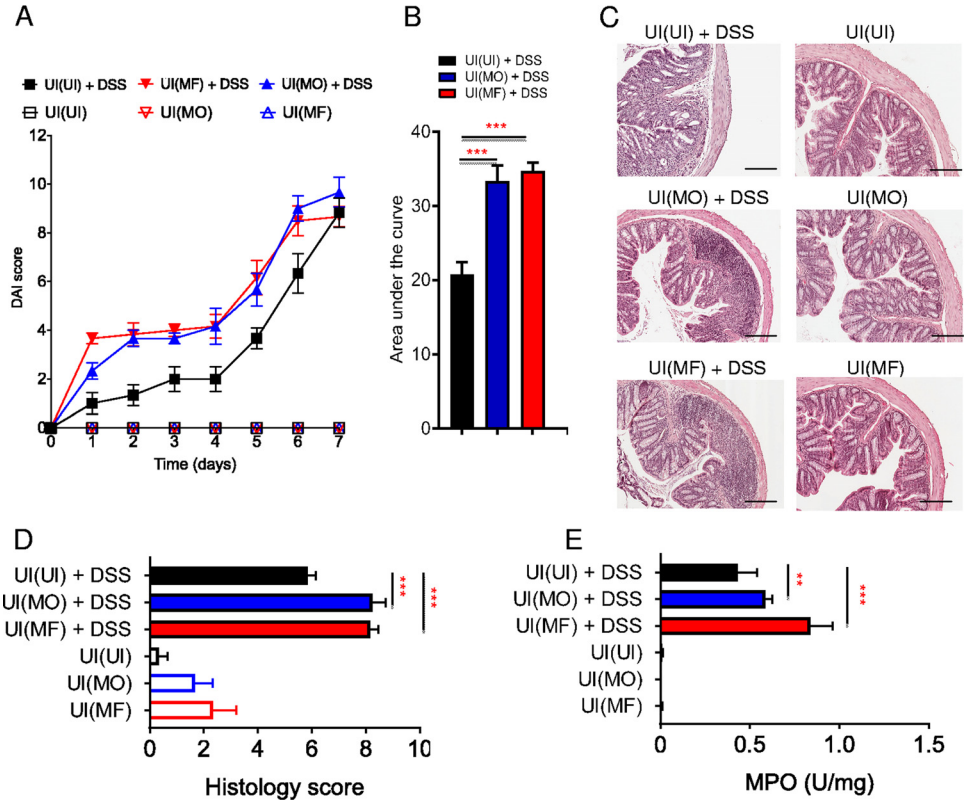

FIG 6 Development of DSS-induced colitis in mice colonized with microbiota from *S. mansoni*-infected mice. (A) Disease activity index (DAI) score for uninfected and antibiotic-treated microbiome recipient mice cohoused with MO-infected [UI(MO)] or MF-infected [UI(MF)] mice or uninfected controls [UI(UI)] receiving DSS (filled symbols) or water (open symbols) (6 mice per group). (B) Area under the curve of DAI groups. (C) Representative H&E-stained histological sections of distal colon samples for the indicated groups (6 mice per group). (D and E) Histological score of distal colon samples and myeloperoxidase (MPO) activity for the indicated groups. Data are representative of >3 separate experiments and are presented as means ± SEM. Statistical difference between groups was determined using two-way ANOVA (A) or one-way ANOVA (B, C, and D) with Tukey's multiple-comparison test. **, $P < 0.01$; ***, $P < 0.001$. Scale bar, 200 μm.

were significantly ($P < 0.001$) increased in both the UI(MF) and UI(MO) groups compared to the levels in UI(UI) mice (Fig. 5E). In contrast, the potentially protective *Lactobacillus* was significantly ($P < 0.001$) reduced in recipients of the microbiota of helminth-infected mice (Fig. 5E). Therefore, cohousing with MO- and MF-infected mice transfers a disrupted intestinal microbiota to recipients. Interestingly, while UI and UI(UI) mice had similar microbiome compositions, there was an evident increase in the abundance of *Bacteroides* and *Parabacteroides* in UI(MF) and UI(MO) mice compared to levels in MF- and MO-infected mice, respectively (Fig. 4C and 5C). These differences provide evidence that further strengthen the hypothesis that *S. mansoni*-infected mice harbor a colitogenic microbiome since when their microbiome is transferred to uninfected mice, potentially colitogenic genera become more abundant in the recipients.

Potentially colitogenic microbiome of *S. mansoni*-infected mice is kept in check by live *S. mansoni* worms. The changes in microbial species following cohousing of microbiome recipients with *S. mansoni*-infected mice indicate that these mice harbor a colitogenic microbiome. To address whether this disrupted microbiota was functional and influenced the development of colitis, we treated microbiome-recipient mice with DSS. During DSS treatment, both UI(MO) and UI(MF) mice developed exacerbated colitis compared to that in UI(UI) mice during the disease course ($P < 0.001$), which was especially noticeable in early stages of DSS-induced colon damage (Fig. 6A and B). Histological examination of the distal colon (Fig. 6C) showed significantly increased ($P < 0.01$ to 0.001) tissue damage in colons of DSS-treated UI(MO) and UI(MF) mice

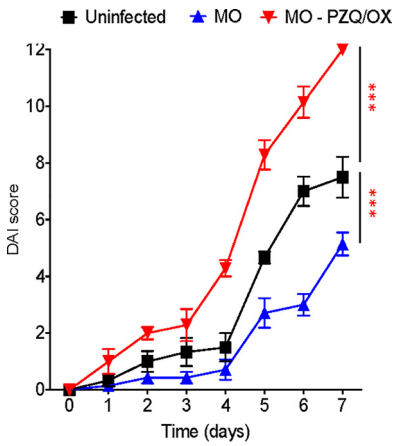

FIG 7 Exacerbated DSS-induced colitis in mice infected with male-only *S. mansoni* worms following anthelmintic treatment. Disease activity index (DAI) score of DSS-exposed MO-infected mice that were untreated or pretreated 8 weeks postinfection with anthelmintic praziquantel (300 mg/kg) and oxamniquine (200 mg/kg) (PZQ-OX) daily for 4 days orally to remove worms. Uninfected DSS-treated mice were used as controls (6 to 7 mice per group). Data are representative of 2 independent experiments and are presented as means ± SEM. Statistical difference in the values between uninfected mice and other groups for the DAI area under the curve was determined using two-way ANOVA followed by Tukey's multiple-comparison test. ***, $P < 0.001$.

compared to that in UI(UI) mice (Fig. 6D), with increased MPO activity in recipients of microbiome from infected mice (Fig. 6E).

In order to assess the functional significance of a live worm infection influencing the intestinal microbiome, MO-infected mice were treated with the anthelmintic drugs praziquantel (PZQ) and oxamniquine (OX) to expel worms prior to exposure to DSS. Interestingly, while MO-infected mice showed reduced susceptibility to DSS-induced colitis, as also shown above (Fig. 1A), following treatment with PZQ-OX, mice developed more severe colitis (Fig. 7). These data indicate that the presence of *S. mansoni* adult male worms continuously modulates the host's intestinal microbiome, preventing the emergence of colitogenic microbiota.

DISCUSSION

In our study, we have demonstrated that infection of mice with *Schistosoma mansoni* dramatically alters the composition of the host intestinal microbiome toward a colitogenic microbiome. Recent studies have highlighted the importance of the intestinal microbiome in colitis as well as its modulation by helminth infections (10–12, 19). We investigated the relationship between two types of experimental *S. mansoni* worm infections, revealing differences between the type of infection in the susceptibility to experimental colitis and the composition of the intestinal microbiota. Mice infected with male *S. mansoni* adult worms are less susceptible to disease in the DSS-induced colitis model, as previously shown (7). Surprisingly, the microbiome of male-*S. mansoni*-infected mice is similar to the microbiome of uninfected control animals. In contrast, in mice infected with conventional male and female worms, with egg deposition leading to intestinal egg granulomatous inflammation and a disrupted intestinal gut barrier, the intestinal microbiome had attributes similar to that of DSS-treated mice, reflecting a colitogenic microbiome. A similar dysbiosis as described here in the intestinal microbiota of MF-infected mice after egg laying and the associated intestinal egg granuloma formation were described previously (20). Indeed, there are supporting data showing that an intact intestinal host microbiota is required during *S. mansoni* infection of mice (21). *S. mansoni*-dependent modulation of the intestinal microbiome is an important but not fully explored parameter that greatly influences the host's pathophysiology during infection.

It was not expected that both MO- and MF-infected mice harbor a transferable microbiome that, in the absence of live adult helminths, exacerbated DSS-induced

colitis in recipient mice. Importantly, anthelmintic treatment of MO-infected mice resulted in loss of protection from colitis, with these mice developing markedly exacerbated disease. We have not examined changes in the microbiome of uninfected mice or male-worm-infected mice after anthelmintic administration. In a previous study in *Schistosoma haematobium*-infected children, while there was significant alteration of the host's microbiome composition during infection, the administration of praziquantel to uninfected children did not result in microbiome differences compared to baseline measurements (22). Further, in a recent study it has been shown that the presence of certain bacterial genera pretreatment may influence praziquantel efficacy (23). Therefore, the praziquantel/oxamniquine treatment regime used is unlikely to have a direct effect on the gut microbiome. These results highlight that continued presence of *S. mansoni* live adult male worms is needed to maintain homeostasis during infection, including control of the potential overgrowth of intestinal pathobionts.

While we have focused on male-only infections, a recent study reported that infection of mice with female-only adult worms (FO) resulted in reduced proinflammatory cytokine production compared to that with male-only adult worm (MO) infections (24). Further investigation is required on *S. mansoni* female-only adult worm infection modulation of the microbiome and intestinal inflammation.

It has been shown that chronic infection with *Heligmosomoides polygyrus* increased short-chain fatty acid production, with the transfer of the modified microbiota giving protection from allergic airway inflammation (25). Previous metabolomic studies of *S. mansoni*-infected mice revealed alterations in the metabolite profiles of infected mice (26). Further studies are required to dissect if alterations in the intestinal microbiota during infections with *S. mansoni* impact the host's metabolism and immunity.

Our study demonstrates that *Schistosoma* worm infection simultaneously modulates the host's immune system and intestinal microbiota and can ameliorate bystander inflammatory colitis. These results further expand our understanding of helminth-host and helminth-microbiota interactions and could benefit anthelmintic and helminth-based therapy development alike.

MATERIALS AND METHODS

Mice and parasitology. BALB/c mice were bred in-house in the Bioresources Unit (Trinity College, Dublin, Ireland). All mice were bred in a specific-pathogen-free barrier facility, with female mice used at 8 to 10 weeks of age.

A Puerto Rican strain of *S. mansoni* was maintained by passage in BALB/c strain mice and albino *Biomphalaria glabrata* snails, as previously described (27). Conventional mixed male and female (MF) sex infections of mice involved use of cercariae shed from infected snails. To prepare snails with male-only-worm (MO) infections, individual snails were exposed to a single *S. mansoni* miracidium. Cercariae from each individual snail were shed and sexed by PCR, as previously described (13). Female 6- to 8-week-old mice were infected percutaneously with 60 male cercariae for MO infections and 30 male and female cercariae for MF infections. Serum IgG responses to adult worm antigen (AW) and soluble egg antigen (SEA) were performed as previously described (28). To remove male worms from infected mice, an anthelmintic combination of praziquantel (PZQ; Bayer AG) and oxamniquine (OX; Pfizer) was used (29). PZQ (300 mg/kg) and OX (200 mg/kg) were administered daily for 4 days orally to mice in an aqueous solution with 2.5% Cremophor EL. Mice were treated at 8 weeks postinfection. To confirm the efficacy of anthelmintic removal of adult worms, untreated and PZQ-OX-treated infected mice were subjected to portal perfusion.

Ethics statement. All animal care and experimental procedures were performed under an Irish Department of Health and Children License (holder Padraic Fallon, license number B100/3250) in compliance with Irish Medicine Board regulations. Animal experiments received ethical approval from the Trinity College Dublin Bioresources Ethical Review Board (reference no. 121108).

DSS-induced colitis. Colitis induction was achieved as previously described (7). Briefly, mice received a 5% solution of DSS (35,000 to 50,000 Da; MP Biomedicals) in their drinking water. Fresh DSS solution was provided every other day for a total of 7 days. The mice were scored daily, and their weights were recorded. Induction of colitis was quantified based on the disease activity index (DAI) as previously described (7). The DAI was calculated for each mouse daily based on three parameters, with a score of 1 to 4 given for each parameter and a maximum cumulative DAI score of 12. Scores were assigned as follows: 0, no weight loss, normal stool, and no blood; 1, 1 to 3% weight loss; 2, 3 to 6% weight loss, loose stool, and blood visible in stool; 3, 6 to 9% weight loss; 4, $>$9% weight loss, diarrhea, and gross breeding. Blood in feces was detected using a Hemdetect occult blood detection kit (Dipro). Colon length was assessed upon termination of the experiments.

Histology. Colon length was measured, and a 1-cm sample from distal colon was fixed in 10% neutral buffered formalin. Following fixation, samples were processed in paraffin wax, sectioned (5-μm thickness), and stained by hematoxylin and eosin (H&E). Histology scoring was performed in a blinded

fashion as previously described (7). Images were acquired using a Leica Microsystems DM3000 LED microscope with an attached DFC495 camera; image analysis was performed on LAS, version 4.0, software (Leica Microsystems).

Cell stimulation and cytokine detection. Following isolation of mesenteric lymph nodes and generation of single-cell suspensions, 1×10^6 cells were stimulated *in vitro* with phorbol-myristate-acetate/ionomycin (PMA/I; Sigma) (50 ng/ml and 500 ng/ml, respectively). After 72 h, supernatants were collected, and IL-10, IL-4, IFN-γ, and IL-17A were detected by enzyme-linked immunosorbent assay (ELISA; R&D Systems), according to the manufacturer's instructions.

Myeloperoxidase activity. Colons were homogenized in a buffer containing phosphate-buffered saline (PBS), 2% fetal bovine serum, and 0.5% cetyltrimethylammonium bromide. Colon protein was determined by a bicinchoninic acid (BCA) assay kit (Thermo Scientific). MPO enzymatic activity was detected using *o*-phenylenediamine as the substrate, and data were interpolated from an MPO (Sigma-Aldrich, UK) standard curve. MPO was expressed as units of enzymatic activity per milligram of colon protein.

Ki-67 staining and TUNEL assay. Colon epithelium cell proliferation was quantified by immunostaining for the detection of the nuclear protein Ki-67 as previously described (30). Briefly, paraffin-embedded sections were hydrated and blocked with 10% normal goat serum (DakoCytomation), followed by overnight incubation with rabbit polyclonal anti-Ki-67 antibody (Abcam). Visualization of Ki-67 staining was performed with an EnVision Detection System (DakoCytomation), and slides were counterstained with Mayer's hematoxylin (Sigma-Aldrich). Late-apoptotic cells were visualized on paraffin-embedded sections using a TUNEL assay (*In Situ* Cell Death Detection kit; Roche, Germany) according to the manufacturer's instructions and as previously described (30). Scoring for the identification of colon epithelial cells undergoing proliferation or apoptosis was performed by enumeration of Ki-67- or TUNEL-positive cells, respectively. Colon sections (2 to 3 sections per mouse and 6 mice per group) were divided in 5 to 6 high-power fields, and the first fully formed 6 to 8 crypts were selected for counting Ki-67- or TUNEL-positive cells. Sections were imaged using a Leica microscope (Leica DM 3000 LED) equipped with a Leica DFC495 camera (Leica Microsystems).

Intestinal permeability. To assess intestinal permeability, mice were gavaged with 0.5 mg/g body weight of fluorescein isothiocyanate-conjugated dextran (FITC-dextran; molecular mass, 4 kDa [Sigma]) administered in sterile PBS. After 4 h, plasma was recovered, and levels of FITC were detected and interpolated with a standard curve, as previously described (31).

Bacterial community analysis. Composition of intestinal microbiota was assessed as previously described (32). Each group of mice was housed together in order to eliminate cage-related effects in microbiome data analysis. Briefly, DNA was extracted from fecal pellets, and the V4 region of the 16S rRNA gene was amplified. Sequencing of the V4 amplicons was performed using a 454 Genome Sequencer FLX Titanium platform (Roche Diagnostics). Quality trimming of the resulting sequencing reads was performed according to previously described criteria (32). Briefly, the following criteria were applied using QIIME: (i) two mismatches were allowed in barcode sequences; (ii) reads could not begin with ambiguous bases (Ns); (iii) read lengths must fall within the range of 150 to 350 bp; and (iv) the minimum average quality score must be at least 25. Chimeric sequences were identified and removed on a per-sample basis using chimera.uchime of the Mothur project (33). Two-stage clustering of sequence reads into operational taxonomic units (OTUs) at 97% similarity was performed. Subsequently, unweighted UniFrac distances were generated based on a rarefied OTU table and resulting phylogeny. A binary and a Spearman distance matrix were generated from a binary OTU table and a normalized OTU table, respectively. Principal coordinate analyses (PCoA) were performed on each of these distance matrices, with box size *d* of 0.05. Permutational multivariate analysis of variance was used to determine whether significant differences existed between subsets of the data, and statistical analysis was performed using DESeq from the DESeq2 R library (34).

Antibiotic treatment and microbiota transfer by cohousing. Mice were treated with a broad-spectrum antibiotic protocol, as described previously (35, 36). Briefly, sex- and age-matched uninfected (UI) mice were treated daily for 10 consecutive days by oral gavage with vancomycin (0.5 mg/ml), neomycin (1 mg/ml), metronidazole (1 mg/ml), ampicillin (1 mg/ml), and gentamicin (1 mg/ml) (Sigma-Aldrich) prepared in 0.2 ml of autoclaved water. Microbiota transfer was achieved by cohousing antibiotic-treated WT mice with MO- or MF-infected mice for 3 weeks. Control microbiota transfer was performed by cohousing antibiotic-treated WT mice with UI mice.

Statistical analysis. Data are expressed as means $\pm$ standard errors of the means (SEM) and were analyzed by analysis of variance (ANOVA) test or unpaired Student's *t*-tests (Prism 6; GraphPad Software). Significance for all statistical tests is described in the figure legends.

SUPPLEMENTAL MATERIAL

Supplemental material for this article may be found at https://doi.org/10.1128/IAI.00275-19.

SUPPLEMENTAL FILE 1, PDF file, 0.1 MB.

SUPPLEMENTAL FILE 2, PDF file, 0.1 MB.

SUPPLEMENTAL FILE 3, PDF file, 0.04 MB.

ACKNOWLEDGMENTS

This work was supported by Science Foundation Ireland (10/IN.1/B3004).

We are grateful for the assistance of Sean Saunders, Emily Hams and Adnan Khan.

REFERENCES

1. World Health Organization. 2019. Schistosomiasis. https://www.who.int/news-room/fact-sheets/detail/schistosomiasis.
2. Pearce EJ, MacDonald AS. 2002. The immunobiology of schistosomiasis. Nat Rev Immunol 2:499–511. https://doi.org/10.1038/nri843.
3. Khan AR, Fallon PG. 2013. Helminth therapies: translating the unknown unknowns to known knowns. Int J Parasitol 43:293–299. https://doi.org/10.1016/j.ijpara.2012.12.002.
4. Fallon PG, Mangan NE. 2007. Suppression of TH2-type allergic reactions by helminth infection. Nat Rev Immunol 7:220–230. https://doi.org/10.1038/nri2039.
5. Schwartz C, Fallon PG. 2018. Schistosoma "eggs-iting" the host: granuloma formation and egg excretion. Front Immunol 9:2492. https://doi.org/10.3389/fimmu.2018.02492.
6. Hams E, Aviello G, Fallon PG. 2013. The schistosoma granuloma: friend or foe? Front Immunol 4:89. https://doi.org/10.3389/fimmu.2013.00089.
7. Smith P, Mangan NE, Walsh CM, Fallon RE, McKenzie AN, van Rooijen N, Fallon PG. 2007. Infection with a helminth parasite prevents experimental colitis via a macrophage-mediated mechanism. J Immunol 178:4557–4566. https://doi.org/10.4049/jimmunol.178.7.4557.
8. Levy M, Kolodziejczyk AA, Thaiss CA, Elinav E. 2017. Dysbiosis and the immune system. Nat Rev Immunol 17:219–232. https://doi.org/10.1038/nri.2017.7.
9. Gilbert JA, Blaser MJ, Caporaso JG, Jansson JK, Lynch SV, Knight R. 2018. Current understanding of the human microbiome. Nat Med 24:392–400. https://doi.org/10.1038/nm.4517.
10. Gause WC, Maizels RM. 2016. Macrobiota—helminths as active participants and partners of the microbiota in host intestinal homeostasis. Curr Opin Microbiol 32:14–18. https://doi.org/10.1016/j.mib.2016.04.004.
11. Harris NL, Loke P. 2017. Recent advances in type-2-cell-mediated immunity: insights from helminth infection. Immunity 47:1024–1036. https://doi.org/10.1016/j.immuni.2017.11.015.
12. Loke P, Lim Y. 2015. Can helminth infection reverse microbial dysbiosis? Trends Parasitol 31:534–535. https://doi.org/10.1016/j.pt.2015.10.001.
13. Smith P, Walsh CM, Mangan NE, Fallon RE, Sayers JR, McKenzie AN, Fallon PG. 2004. Schistosoma mansoni worms induce anergy of T cells via selective up-regulation of programmed death ligand 1 on macrophages. J Immunol 173:1240–1248. https://doi.org/10.4049/jimmunol.173.2.1240.
14. Mangan NE, Fallon RE, Smith P, van Rooijen N, McKenzie AN, Fallon PG. 2004. Helminth infection protects mice from anaphylaxis via IL-10-producing B cells. J Immunol 173:6346–6356. https://doi.org/10.4049/jimmunol.173.10.6346.
15. Nagalingam NA, Kao JY, Young VB. 2011. Microbial ecology of the murine gut associated with the development of dextran sodium sulfate-induced colitis. Inflamm Bowel Dis 17:917–926. https://doi.org/10.1002/ibd.21462.
16. Perse M, Cerar A. 2012. Dextran sodium sulphate colitis mouse model: traps and tricks. J Biomed Biotechnol 2012:718617. https://doi.org/10.1155/2012/718617.
17. Dziarski R, Park SY, Kashyap DR, Dowd SE, Gupta D. 2016. *Pglyrp*-regulated gut microflora Prevotella falsenii, Parabacteroides distasonis and Bacteroides eggerthii enhance and Alistipes finegoldii attenuates colitis in mice. PLoS One 11:e0146162. https://doi.org/10.1371/journal.pone.0146162.
18. Coccia M, Harrison OJ, Schiering C, Asquith MJ, Becher B, Powrie F, Maloy KJ. 2012. IL-1beta mediates chronic intestinal inflammation by promoting the accumulation of IL-17A secreting innate lymphoid cells and $CD4^+$ Th17 cells. J Exp Med 209:1595–1609. https://doi.org/10.1084/jem.20111453.
19. Lee SC, Tang MS, Lim YA, Choy SH, Kurtz ZD, Cox LM, Gundra UM, Cho I, Bonneau R, Blaser MJ, Chua KH, Loke P. 2014. Helminth colonization is associated with increased diversity of the gut microbiota. PLoS Negl Trop Dis 8:e2880. https://doi.org/10.1371/journal.pntd.0002880.
20. Jenkins TP, Peachey LE, Ajami NJ, MacDonald AS, Hsieh MH, Brindley PJ, Cantacessi C, Rinaldi G. 2018. Schistosoma mansoni infection is associated with quantitative and qualitative modifications of the mammalian intestinal microbiota. Sci Rep 8:12072. https://doi.org/10.1038/s41598-018-30412-x.
21. Holzscheiter M, Layland LE, Loffredo-Verde E, Mair K, Vogelmann R, Langer R, Wagner H, Prazeres da Costa C. 2014. Lack of host gut microbiota alters immune responses and intestinal granuloma formation during schistosomiasis. Clin Exp Immunol 175:246–257. https://doi.org/10.1111/cei.12230.
22. Kay GL, Millard A, Sergeant MJ, Midzi N, Gwisai R, Mduluza T, Ivens A, Nausch N, Mutapi F, Pallen M. 2015. Differences in the faecal microbiome in Schistosoma haematobium infected children vs. uninfected children. PLoS Negl Trop Dis 9:e0003861. https://doi.org/10.1371/journal.pntd.0003861.
23. Schneeberger PHH, Coulibaly JT, Panic G, Daubenberger C, Gueuning M, Frey JE, Keiser J. 2018. Investigations on the interplays between Schistosoma mansoni, praziquantel and the gut microbiome. Parasit Vectors 11:168. https://doi.org/10.1186/s13071-018-2739-2.
24. Sombetzki M, Koslowski N, Rabes A, Seneberg S, Winkelmann F, Fritzsche C, Loebermann M, Reisinger EC. 2018. Host defense versus immunosuppression: unisexual infection with male or female Schistosoma mansoni differentially impacts the immune response against invading cercariae. Front Immunol 9:861. https://doi.org/10.3389/fimmu.2018.00861.
25. Zaiss MM, Rapin A, Lebon L, Dubey LK, Mosconi I, Sarter K, Piersigilli A, Menin L, Walker AW, Rougemont J, Paerewijck O, Geldhof P, McCoy KD, Macpherson AJ, Croese J, Giacomin PR, Loukas A, Junt T, Marsland BJ, Harris NL. 2015. The intestinal microbiota contributes to the ability of helminths to modulate allergic inflammation. Immunity 43:998–1010. https://doi.org/10.1016/j.immuni.2015.09.012.
26. Wang Y, Holmes E, Nicholson JK, Cloarec O, Chollet J, Tanner M, Singer BH, Utzinger J. 2004. Metabonomic investigations in mice infected with Schistosoma mansoni: an approach for biomarker identification. Proc Natl Acad Sci U S A 101:12676–12681. https://doi.org/10.1073/pnas.0404878101.
27. Khan AR, Amu S, Saunders SP, Fallon PG. 2014. The generation of regulatory B cells by helminth parasites. Methods Mol Biol 1190:143–162. https://doi.org/10.1007/978-1-4939-1161-5_11.
28. Fallon PG, Dunne DW. 1999. Tolerization of mice to Schistosoma mansoni egg antigens causes elevated type 1 and diminished type 2 cytokine responses and increased mortality in acute infection. J Immunol 162:4122–4132.
29. Fallon PG, Fookes RE, Wharton GA. 1996. Temporal differences in praziquantel- and oxamniquine-induced tegumental damage to adult Schistosoma mansoni: implications for drug-antibody synergy. Parasitology 112:47–58. https://doi.org/10.1017/S0031182000065069.
30. Aviello G, Corr SC, Johnston DG, O'Neill LA, Fallon PG. 2014. MyD88 adaptor-like (Mal) regulates intestinal homeostasis and colitis-associated colorectal cancer in mice. Am J Physiol Gastrointest Liver Physiol 306:G769–G778. https://doi.org/10.1152/ajpgi.00399.2013.
31. Corr SC, Palsson-McDermott EM, Grishina I, Barry SP, Aviello G, Bernard NJ, Casey PG, Ward JB, Keely SJ, Dandekar S, Fallon PG, O'Neill LA. 2014. MyD88 adaptor-like (Mal) functions in the epithelial barrier and contributes to intestinal integrity via protein kinase C. Mucosal Immunol 7:57–67. https://doi.org/10.1038/mi.2013.24.
32. Jeffery IB, Lynch DB, O'Toole PW. 2016. Composition and temporal stability of the gut microbiota in older persons. ISME J 10:170–182. https://doi.org/10.1038/ismej.2015.88.
33. Schloss PD. 2009. A high-throughput DNA sequence aligner for microbial ecology studies. PLoS One 4:e8230. https://doi.org/10.1371/journal.pone.0008230.
34. Love MI, Huber W, Anders S. 2014. Moderated estimation of fold change and dispersion for RNA-seq data with DESeq2. Genome Biol 15:550. https://doi.org/10.1186/s13059-014-0550-8.
35. Hill DA, Hoffmann C, Abt MC, Du Y, Kobuley D, Kirn TJ, Bushman FD, Artis D. 2010. Metagenomic analyses reveal antibiotic-induced temporal and spatial changes in intestinal microbiota with associated alterations in immune cell homeostasis. Mucosal Immunol 3:148–158. https://doi.org/10.1038/mi.2009.132.
36. Floudas A, Saunders SP, Moran T, Schwartz C, Hams E, Fitzgerald DC, Johnston JA, Ogg GS, McKenzie AN, Walsh PT, Fallon PG. 2017. IL-17 receptor A maintains and protects the skin barrier to prevent allergic skin inflammation. J Immunol 199:707–717. https://doi.org/10.4049/jimmunol.1602185.